Retroreflecting polarization spectroscopy enabling miniaturization

D. Groswasser,[a] A. Waxman, M. Givon, G. Aviv, Y. Japha, M. Keil, and R. Folman
Department of Physics and Ilse Katz Center for Meso- and Nanoscale Science and Technology, Ben-Gurion University of the Negev, P.O. Box 653, Be'er Sheva 84105, Israel

(Received 9 July 2009; accepted 6 August 2009; published online 3 September 2009)

We describe and characterize alternative configurations for Doppler-free polarization spectroscopy. The suggested apparatus enables complete pump/probe beam overlap and allows substantial miniaturization. Its utility and performance for narrow linewidth, high-stability frequency locking is discussed for the $|5S_{1/2}F=2\rangle \rightarrow |5P_{3/2}F'\rangle D_2$ transition in ^{87}Rb. © *2009 American Institute of Physics.* [doi:10.1063/1.3213076]

I. INTRODUCTION

Polarization spectroscopy is a sensitive Doppler-free spectroscopic method introduced in 1976 by Wieman and Hänsch.[1] It is closely related to saturation spectroscopy[2] and is used in atomic and molecular physics for resolving spectral features obscured by the broad Doppler profile. This technique is commonly applied to laser locking[3–5] where it is important to fix the laser frequency on a specific atomic transition, as in laser cooling, atomic clocks, and atomic magnetometry. Laser locking to an atomic transition is also advantageous for the optical communication industry,[6,7] as it enables standardization, narrow linewidth, and long-term stability. The basic principle is to use a circularly polarized pump beam to polarize the sample, and to probe the polarized sample using a linearly polarized beam. Any rotation of the probe beam polarization due to induced birefringence/optical dichroism is detected using a polarimeter that subtracts the relative intensities of two orthogonal linear polarizations (Fig. 1). Experimental results for Rb and Cs atoms have been simulated by several groups and yield good agreement with theory.[8,9] Polarization spectroscopy is particularly suitable for laser locking since the detected transitions have a natural dispersive lineshape and can readily be used as an input "error" signal to an electronic servo-system that keeps the laser output frequency fixed on the atomic transition. Hence, this technique does not require modulation of the laser light or use of a lock-in amplifier as in frequency modulation spectroscopy,[10] making it favorable also in terms of cost and complexity. Furthermore, we note that in addition to its simplicity, polarization spectroscopy has certain specific properties that make it particularly suitable for miniature laser-locking systems. The differential polarization-detection system provides an inherent common-mode noise rejection feature that makes it less sensitive to fluctuations in the laser intensity or to scattering by fluorescence. In addition, while in Doppler-free saturation spectroscopy the signal results only from absorption, in polarization spectroscopy there is also a significant dispersion contribution. Hence, as already noted,[3,8,11] this technique is favorable for obtaining relatively high signal-to-noise (S/N) ratios in thin or low-pressure samples where absorption is low but dispersion can be significant. Consequentially cell heating may not be required.

However, polarization spectroscopy suffers from several drawbacks. The locking point is very sensitive to external magnetic fields, and therefore magnetic shielding of the atomic sample is required. The capture range of this technique is limited by the power-broadened linewidth of the atomic transitions, which for alkali atoms is typically 10–20 MHz, though this capture range may be extended further.[12] Finally, although variations in the conventional optical setup eliminate the angle between pump and probe beams,[13] the separated beam paths of the linearly polarized probe and circularly polarized pump are not suitable for miniaturization. It is this issue that we address here.

Progress in microelectromechanical systems technology has led to the production of miniature vapor cells[14] and the realization of compact atom-based devices such as the chip-scale atomic clock[15] and the chip-scale atomic magnetometer,[16] both based on coherent population trapping. Miniature vapor cell technology is also essential for compact laser-locking systems based on an atomic reference. Knappe *et al.*[17] fabricated a saturation-absorption laser spectrometer with a volume of 0.1 cm^3 using only off-the-shelf components. They estimated that using miniaturized saturation spectroscopy to lock distributed feedback (DFB) or distributed Bragg reflector (DBR) lasers will reduce laser linewidths to 100 kHz. Moreover, new generations of DFB, DBR, and vertical-cavity surface-emitting lasers are now available with extended wavelength ranges. These lasers are suitable for many applications including spectroscopy, metrology, laser cooling, and optical communication, many of which require wavelength stabilization. Hence, there is considerable motivation for the development of compact laser-locking systems based on atomic standards.

II. EXPERIMENTAL

Here we present several new experimental versions for polarization spectroscopy. In Fig. 2 we describe two "T-shape" schemes that perform just as well as the standard schemes[5,8,9] but with fewer optical components and with complete beam overlap, using only conventional off-the-

[a]Author to whom correspondence should be addressed. Electronic mail: davgros@bgu.ac.il.

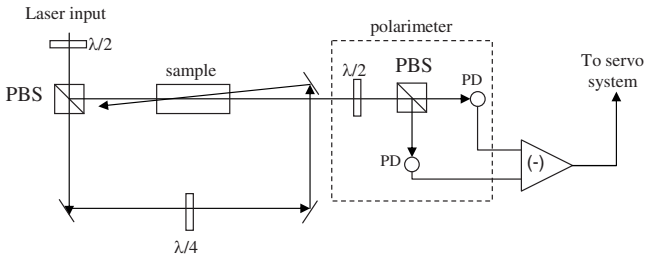

FIG. 1. A standard scheme for polarization spectroscopy. Using a $\lambda/2$ waveplate and a polarizing beamsplitter cube (PBS) the laser beam is divided into pump and probe beams. The pump beam acquires a circular polarization after passing through a $\lambda/4$ waveplate and is then steered by mirrors to pump the sample. The change in the polarization plane of the counterpropagating probe beam due to the induced anisotropy is analyzed by a polarimeter consisting of a $\lambda/2$ waveplate, a PBS, and two photodiodes.

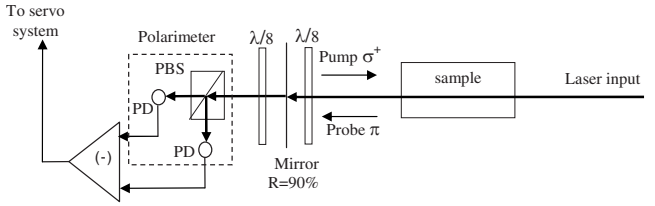

FIG. 3. In this linear configuration the input beam is linearly polarized. A semitransparent mirror retroreflects part of the pump beam, which thereby becomes circularly polarized by twice passing through the $\lambda/8$ waveplate. The transmitted part of the beam, which is elliptically polarized, passes through a second $\lambda/8$ waveplate rotated by 90° with respect to the axes of the first waveplate to reverse its retardation effect. The probe light is analyzed by the polarimeter, which as described in the text, may also be made to function without a beamsplitter, thereby enabling a completely planar construction.

shelf components. An even more compact "linear" setup is described in Fig. 3. This completely one-dimensional setup, which does not require a beamsplitter, enables planar fabrication and therefore monolithic integration to achieve extreme miniaturization.

Residual magnetic fields near the sample cell are reduced by a single layer of mu-metal shielding to about 0.08 G. The laser power of the pump and probe beams is kept at $10-15\ \mu W/mm^2$, with the probe beams somewhat weaker than the pump beams for the T-shape configurations and the reverse for the linear configuration. In all cases, the beam radius is about 1 mm.

The main advantage of the new configurations is that the incoming laser beam is not split into pump and probe beams as in the conventional setup (Fig. 1). Instead, in the T-shape configurations (Fig. 2), the incoming beam is circularly polarized by a $\lambda/4$ waveplate and directed toward the sample (in our case, a ^{87}Rb vapor cell) to serve as the "pump" beam. The beam is then reflected back through the sample toward the polarimeter. This is the "probe" beam. The conversion from circularly polarized pump to linearly polarized probe can be achieved either by a polarizer or by a double pass through a $\lambda/8$ waveplate. The configuration using the linear polarizer is easily understood: the polarizer passes only one linear component of the circularly polarized pump beam back toward the cell and the polarimeter. The angle of the polarizer is chosen to balance the polarimeter (Fig. 2). Alternatively, the circular polarization of the pump beam is converted to linear polarization following retroreflection and double passage through a $\lambda/8$ waveplate. Again, this waveplate is rotated to balance the polarimeter.

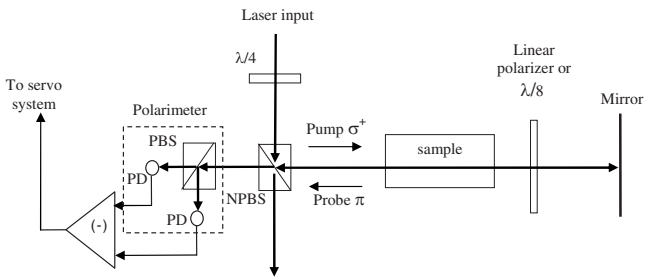

FIG. 2. Schematic layout of the suggested T-shape configurations. The incoming laser beam is circularly polarized by a $\lambda/4$ waveplate. This pump beam is directed to the sample by a non-PBS cube (NPBS) and optically pumps it. After exiting the sample, the pump beam becomes linearly polarized either by a polarizer or by twice passing through a $\lambda/8$ waveplate. The probe beam travels back through the sample and the NPBS to reach the polarimeter.

In the linear configuration (Fig. 3) the linearly polarized input beam probes the sample as it passes through the cell toward the polarimeter. In order to polarize the sample, part of the light is retroreflected by a semitransparent mirror, consequently passing twice through a $\lambda/8$ waveplate and thereby becoming circularly polarized. In contrast to the other configurations, the returning pump beam intensity is lower than the probe beam intensity since some of the light is transmitted through the semitransparent mirror to the polarimeter ($R=90\%$). The transmitted light is passed through a second $\lambda/8$ waveplate, which is rotated by 90° with respect to the first waveplate, hence canceling the retardation effect of the first $\lambda/8$ waveplate. Any changes in the polarization plane of the light may therefore be attributed to optical activity in the cell.

The latter linear configuration enables further miniaturization since it is based solely on a stack of planar optical elements. In particular, beamsplitter cubes can be dispensed with altogether by constructing a polarimeter having adjacent photodiodes covered by orthogonally oriented polarizers, each sampling separate halves of the detected beam. Combined with available technology for planar evaporated (i.e., noncrystalline) polarizers and waveplates, and miniature vapor cell technology based on wafer bonding, this construction will reduce the complete locking apparatus to a volume of 1 mm^3.

III. RESULTS AND CONCLUSION

Spectra of the $|5S_{1/2}F=2\rangle \rightarrow |5P_{3/2}F'\rangle$ transition in ^{87}Rb using the two T-shape configurations suggested in Fig. 2 are shown in Figs. 4(a) and 4(b). They are compared to the linear configuration [Fig. 4(c)], to standard polarization spectroscopy [Fig. 4(d)], and to saturation spectroscopy [Fig. 4(e)]. To avoid power broadening, care is taken to ensure that the input beam intensity is lower than the saturation intensity ($16\ \mu W/mm^2$). Very good agreement with the literature is shown for spectra using the T-shape configuration with a linear polarizer [Fig. 4(a)] and for the linear configuration [Fig. 4(c)]. The spectrum using the T-shape configuration

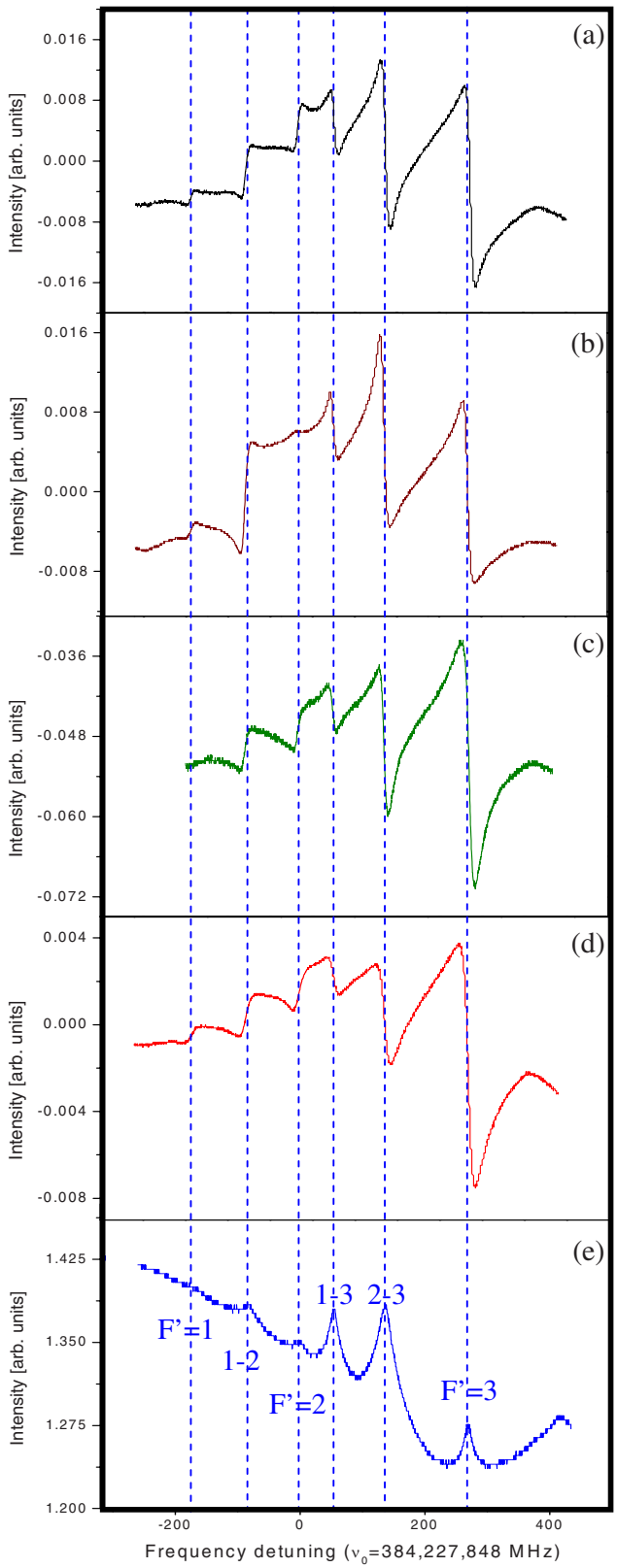

FIG. 4. (Color online) Comparison between spectra obtained by using the suggested polarization spectroscopy T-shape configurations with a polarizer (a) or a $\lambda/8$ waveplate (b), the linear configuration (c), and standard polarization spectroscopy (d). A saturation spectroscopy spectrum (Ref. 2) is presented for reference in (e), where the frequency ν_0 is taken from Steck (Ref. 18) for the $|5S_{1/2}F=2\rangle \rightarrow |5P_{3/2}F'=2\rangle D_2$ transition in ^{87}Rb.

with a $\lambda/8$ waveplate [Fig. 4(b)] is similar to the standard polarization spectroscopy spectrum [Fig. 4(d)], although differences in the detailed structure may be observed.

The T-shape and linear configurations also differ in their pump/probe intensity ratios; for the former this ratio is always >1, whereas it is always <1 for the latter configuration. This suggests that polarization may be incomplete for the linear configuration below the saturation intensity. Nevertheless, for standard Rb cells at room temperature we have demonstrated that the resulting spectra exhibit all spectral features with good S/N ratio and sharp error signals that are suitable for laser locking, just like conventional polarization spectroscopy.

To conclude, we have demonstrated miniaturization-enabling schemes for polarization spectroscopy. The two T-shape configurations perform as well as the standard setup but require fewer optical components. We also describe a linear setup that, in addition, enables planar fabrication. Both configurations are easy to construct and yield complete pump-probe overlap.

ACKNOWLEDGMENTS

We thank the team of the Ben-Gurion University "Atom-Chip" laboratory (www.bgu.ac.il/atomchip). We gratefully acknowledge the support of the European Union, the German Government (DIP Contract No. F.2.2), the French Government, the American-Israeli Foundation (BSF Contract No. 2004078), the Israeli Science Foundation Contract No. 8006/03, and the Ministry of Immigrant Absorption (Israel).

[1] C. Wieman and T. W. Hänsch, Phys. Rev. Lett. **36**, 1170 (1976).
[2] W. Demtröder, *Laser Spectroscopy* (Springer, Berlin, 1998).
[3] Y. Yoshikawa, T. Umeki, T. Mukae, Y. Torii, and T. Kuga, Appl. Opt. **42**, 6645 (2003).
[4] G. P. T. Lancaster, R. S. Conroy, M. A. Clifford, J. Arlt, and K. Dholakia, Opt. Commun. **170**, 79 (1999).
[5] C. P. Pearman, C. S. Adams, S. G. Cox, P. F. Griffin, D. A. Smith, and I. G. Hughes, J. Phys. B **35**, 5141 (2002).
[6] V. Mahal, A. Arie, M. A. Arbore, and M. M. Fejer, Opt. Lett. **21**, 1217 (1996).
[7] F. Ducos, J. Honthaas, and O. Acef, Eur. Phys. J.: Appl. Phys. **20**, 227 (2002).
[8] M. L. Harris, C. S. Adams, S. L. Cornish, I. C. McLeod, E. Tarleton, and I. G. Hughes, Phys. Rev. A **73**, 062509 (2006).
[9] H. Do, G. Moon, and H. Noh, Phys. Rev. A **77**, 032513 (2008).
[10] G. C. Bjorklund, Opt. Lett. **5**, 15 (1980).
[11] T. Petelski, M. Fattori, G. Lamporesi, J. Stuhler, and G. M. Tino, Eur. Phys. J. D **22**, 279 (2003).
[12] A. Ratnapala, C. J. Vale, A. G. White, M. D. Harvey, N. R. Heckenberg, and H. Rubinsztein-Dunlop, Opt. Lett. **29**, 2704 (2004).
[13] V. B. Tiwari, S. Singh, S. R. Mishra, H. S. Rawat, and S. C. Mehendale, Opt. Commun. **263**, 249 (2006).
[14] L. Liew, S. Knappe, J. Moreland, H. Robinson, L. Hollberg, and J. Kitching, Appl. Phys. Lett. **84**, 2694 (2004).
[15] S. Knappe, P. D. D. Schwindt, V. Shah, L. Hollberg, J. Kitching, L. Liew, and J. Moreland, Opt. Express **13**, 1249 (2005).
[16] P. D. D. Schwindt, S. Knappe, V. Shah, L. Hollberg, J. Kitching, L. Liew, and J. Moreland, Appl. Phys. Lett. **85**, 6409 (2004).
[17] S. A. Knappe, H. G. Robinson, and L. Hollberg, Opt. Express **15**, 6293 (2007).
[18] D. A. Steck, Rubidium 87 D Line Data (revision 2.1.1) (2009) (http://steck.us/alkalidata/rubidium87numbers.pdf).